

Simple Distance-based Thread Analytical Device Integrated with Ion Imprinted Polymer for Zn²⁺ Quantification in Human Urine Samples

Lita Chheang,^{a,b,c,d*} Kawin Khachornsakkul,^{a,b*} Ruben Del-Rio-Ruiz,^{a,b} Wenxin Zeng,^{a,b} Nisakorn Thongkon,^c Sudtida Pliankarom Thanasupsin,^e Sameer Sonkusale,^{a,b*}

^aDepartment of Electrical and Computer Engineering, Tufts University, Medford, MA 02155, USA

^bNano Lab, Tufts University, Medford, MA 02155, USA

^cDepartment of Chemistry, Faculty of Science, King Mongkut's University of Technology Thonburi, Bangkok 10140, Thailand

^dDepartment of Chemistry, Faculty of Science, Royal University of Phnom Penh, Federation of Russia Blvd, Tuol Kork, Phnom Penh, Cambodia

^eChemistry for Green Society and Healthy Living Research Unit, Faculty of Science, King Mongkut's University of Technology Thonburi, Bangkok 10140, Thailand

*To whom correspondence should be addressed. Email: lita.chheang@tufts.edu
Kawin.khachornsakkul@tufts.edu sameer.sonkusale@tufts.edu

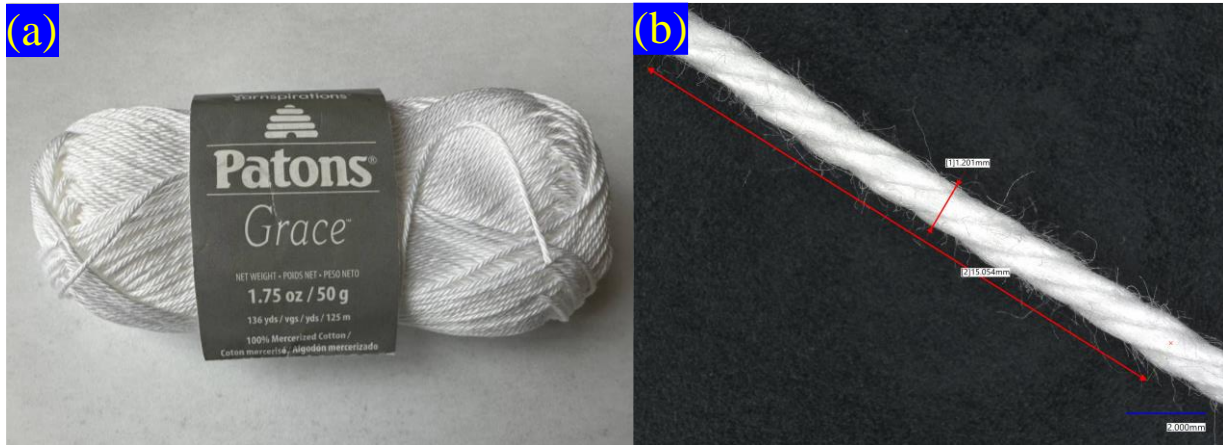


Fig. S1. (a) Cotton thread brand and (b) a strand of the cotton thread was observed under microscopy. The width of the strand is around 1.201 mm and the twist per inch (TPI) parameter of the thread is 15.0 inches.

Design and fabrication of the supportive platform

The platform consisted of a 3D printed part to support the dTADs. The total dimensions of this platform were 16.0 mm, 129.0 mm, and 8.0 mm (width x length x height) with a wall thickness of 3.0 mm, as shown in **Fig. S2**. Its interior containing a printed ruler of 12.0 cm (length) was designed to assist the reagent coating, the sample solution introduction, and the colorimetric distance-based measurement. Besides, both end sides of the platform layer were patterned to acquire the small channels for holding and keeping aligned the cotton thread with the platform (**Fig. S3**). The platform was initially designed with Solidworks and exported to Ultimaker Cura Software to generate the 3D printing layers and supports. Afterwards, the platform was 3D printed with matte black PLA filament using an Ultimaker S5 fused deposition modelling printer (Utrecht, Netherlands). Subsequently, its supports were removed and its surfaces were further polished with sandpaper to acquire a smoother finish. In addition, we can confirm that this manufacturing produces a smooth finish with a good accuracy, around 100.0 μm , as well as a fast fabrication process of 3 hours. Owing to the use of 3D printing, the proposed dTADs for quantitative monitoring of zinc ions provides greater portability, affordability and ease of manufacture and use.

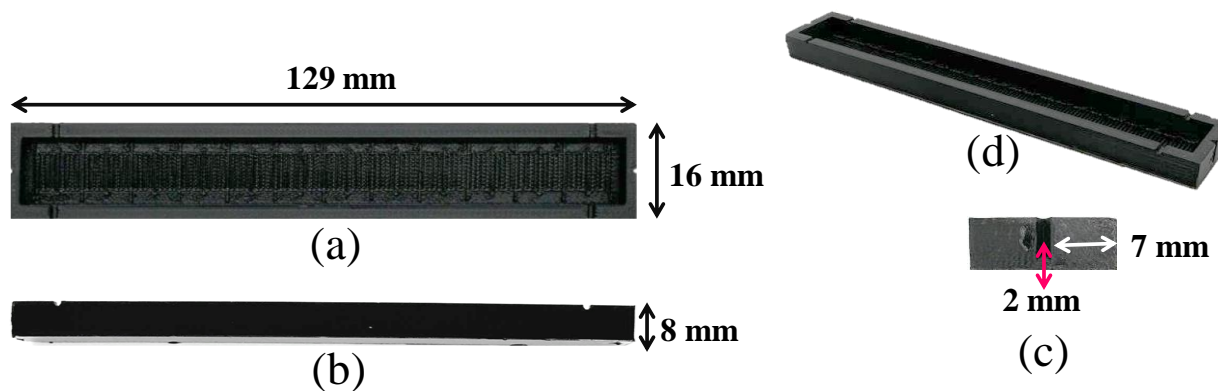


Fig. S2. Dimensions of the fabricated platform, (a) top view, (b) front view, (c) right-side view, and (d) perspective view.

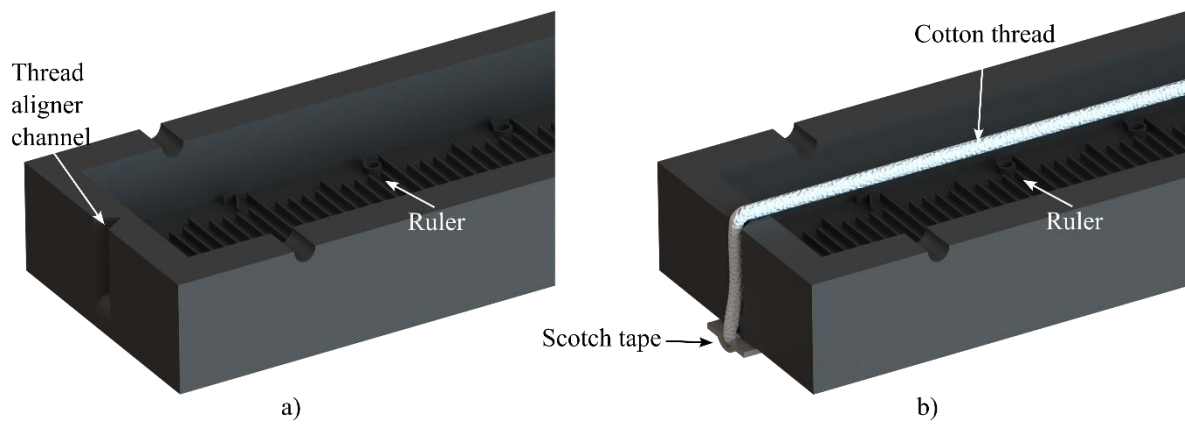


Fig. S3 Left end-side of proposed platform including thread aligner channel and illustrating a) platform with thread aligner channel and 3D printed ruler and b) platform with cotton thread assembled into platform.

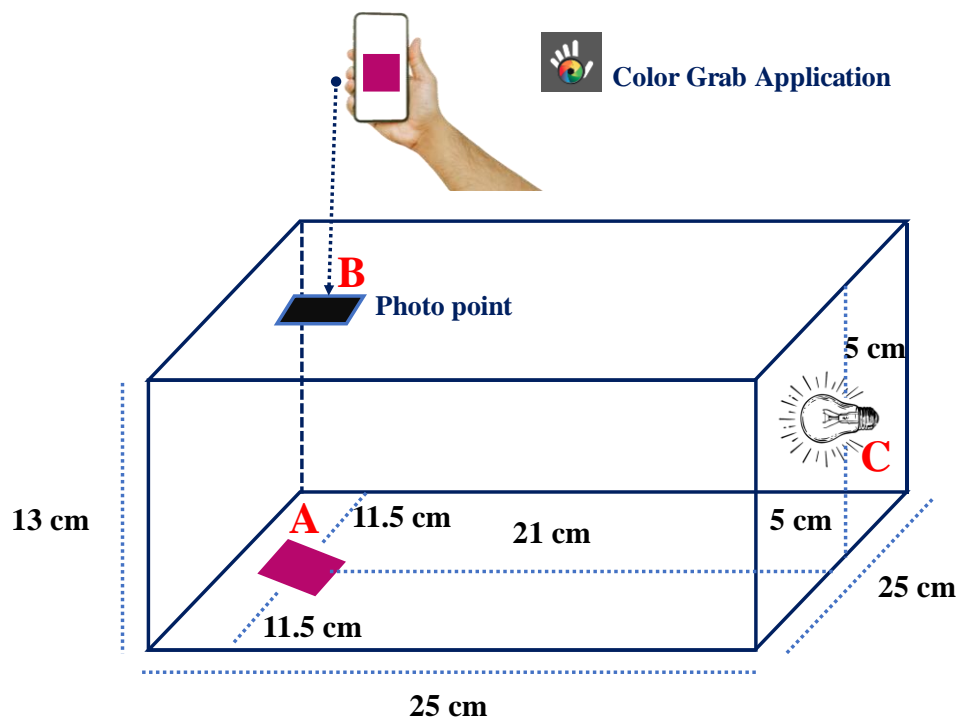


Fig. S4. Device box showing the internal position A: Cotton pad B: Smartphone C: LED lamp.

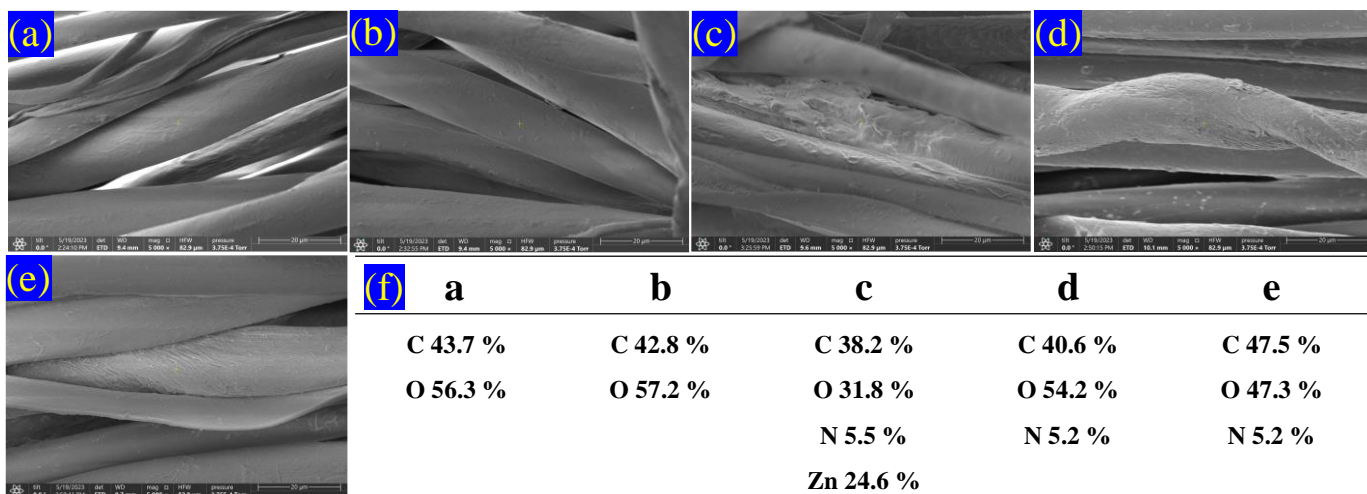


Fig. S5. SEM images (20 μm) obtained at 5 kV acceleration voltage: (a) bare-dTADs, (b) treated-dTADs, (c) Zn-IIPs-based dTADs, (d) IIPs-based dTADs, (e) NIIPs-based dTADs, and (f) EDS analysis of each dTADs.

Characterization of IIPs-based dTADs

The FTIR spectra of complexing ligand (DTZ), monomer (MAA), cross-linker (EGDMA), initiator (AIBN), and the IIP are presented in **Fig. S6**. The absorption bands are identified as follows (**Fig. S6 (a and b)**). The 3660 to 2900 cm^{-1} wavenumber range exhibits distinct peaks attributed to the stretching vibration of polysaccharides' O–H and C–H bonds. The prominent peak observed at 3331 cm^{-1} indicates the stretching vibration associated with the OH group in polysaccharides [1–4]. The FTIR spectra (**Fig. S6 (c, d, and e)**) of MAA exhibit a peak within the wavenumber range of 3200 to 3500 cm^{-1} , which corresponds to the stretching vibrations of the O–H bond attributed to the presence of carboxylic acid. The observed peak at a wavenumber of 2900 cm^{-1} can be attributed to stretching the C–H bonds, specifically those within the methyl group. The observed peak at 1630 cm^{-1} can be attributed to the stretching of the C=O bond, characteristic of the carboxylic group [5,6]. Furthermore, the prominent peak observed at 1724 cm^{-1} in the polymer spectra was attributed to carbonyl groups originating from EGDMA and MAA. The polymer is synthesized through the process of addition reaction, wherein the C=C double bond is added to a single C–C bond and 1145 cm^{-1} (C–O stretching) [7–9]. The stretching vibration band associated with hydrogen-bonded alcohol (O–H) is approximately 3350 cm^{-1} . The ester group's C–O stretching vibration is also detected at 1724 cm^{-1} . Furthermore, an absorption band with a weak shoulder is observed around 2950 cm^{-1} , corresponding to stretching aliphatic –CH, –CH₂, and –CH₃ groups. Multiple spectral bands were seen within the fingerprint region (1600–1000 cm^{-1}) corresponding to ethylene glycol units derived from poly (EGDMA) constituents. The observed peaks corresponded to the scissoring band of –CH₂ groups in ethylene glycol units at a wavenumber of 1480 cm^{-1} and the antisymmetric and symmetric stretching bands of –O–R groups in ethylene glycol units at a wavenumber of 1160 cm^{-1} , respectively [9]. For the spectra of

dithizone adsorption with metal (Zn), the weak adsorption band at 1589 cm^{-1} shows the N=N stretching band, and after treatment with metals, the weak adsorption band moved to 1593 cm^{-1} . The N-H scissor band appeared at 1494 cm^{-1} , but after being treated with metals, the band dropped to 1492 cm^{-1} . The peak at 1435 cm^{-1} is due to the C=S stretching mode. When metal is added to C=S, the peak moves to 1432 cm^{-1} . The peak at 1210 cm^{-1} is due to the deformation of the N-H bond, and its drop to 1203 cm^{-1} is caused by replacing a metal ion for the H ion in one of the N-H bonds in one dithizone molecule [10].

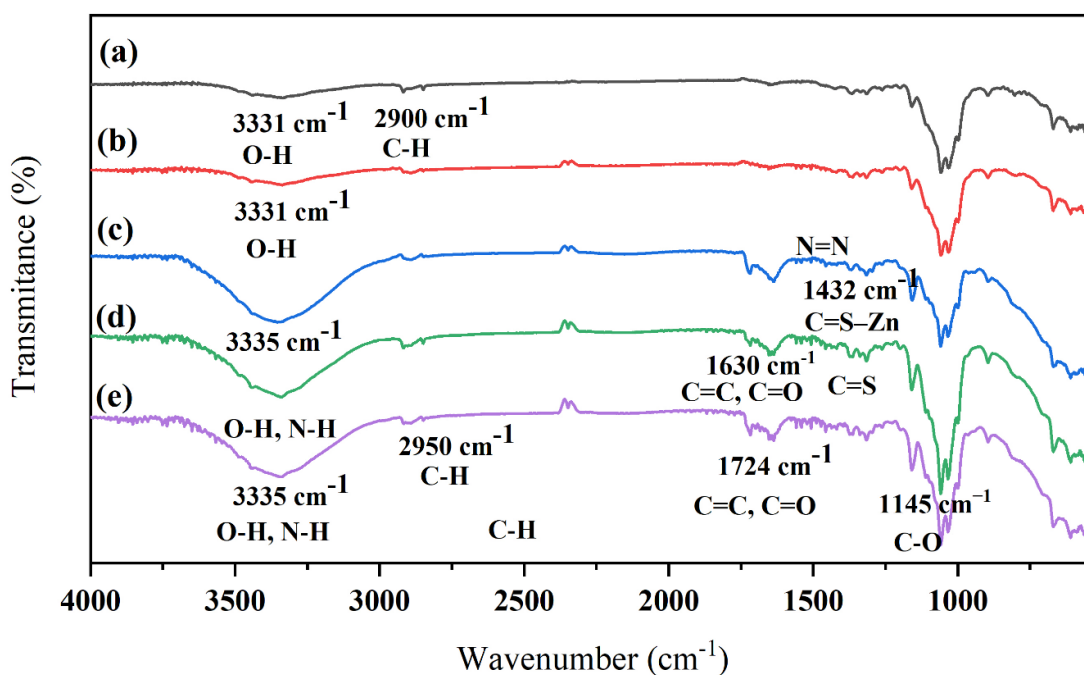


Fig. S6. ATR-FTIR transmission spectra of (a) Bare-dTADs, (b) Treated-dTADs, (c) Zn-IIPs-based dTADs, (d) IIPs-based dTADs, and (e) NIIPs-based dTADs.

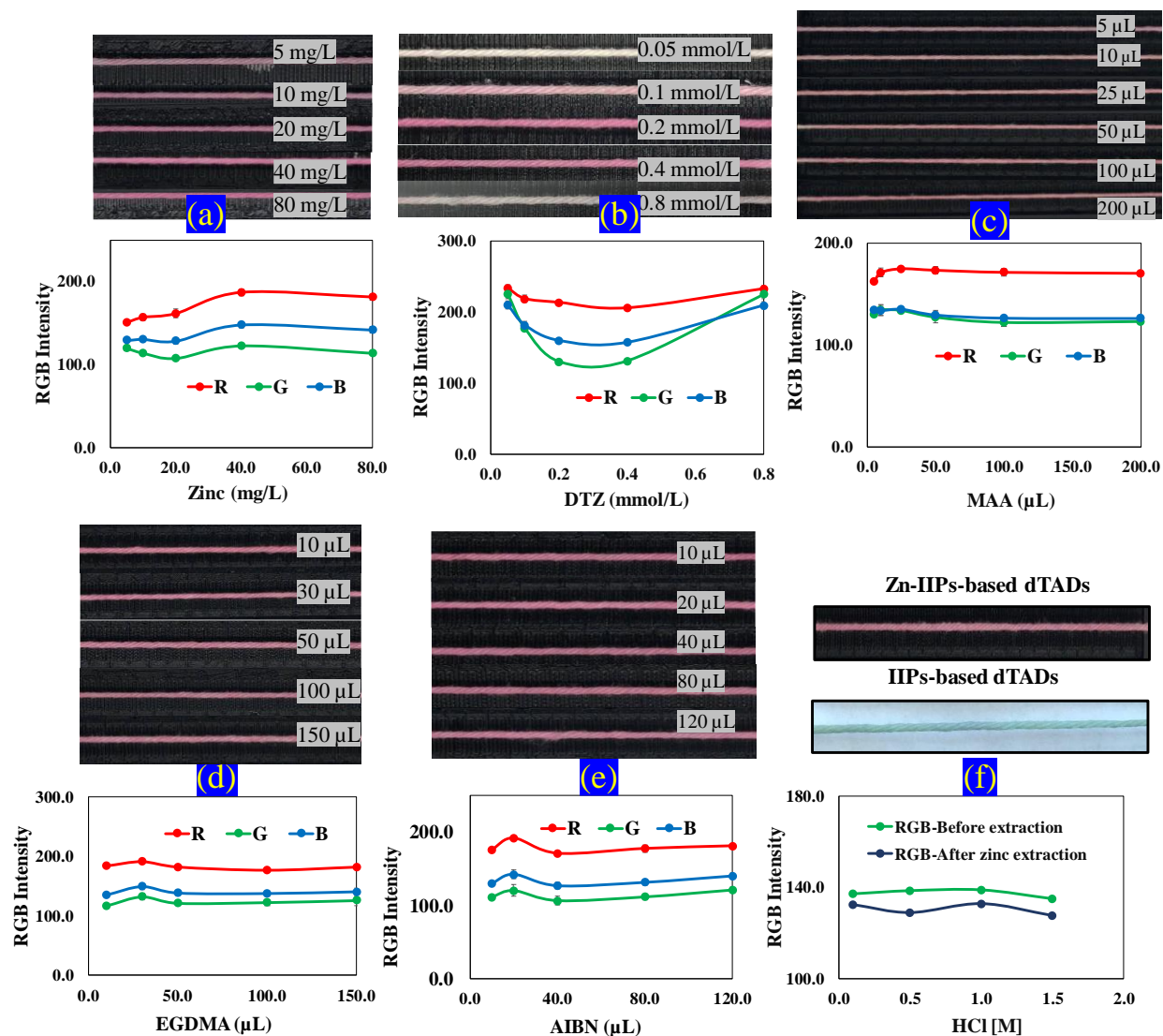


Fig. S7. Graph and image of optimization studies of concentration (a) Zn^{2+} , (b) DTZ, volume (c) MAA, (d) EGDMA, (e) AIBN, and (f) HCl concentration.

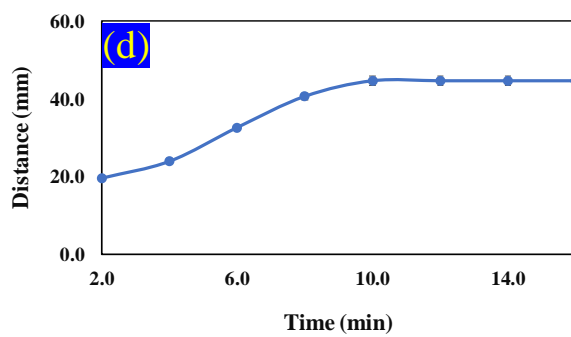
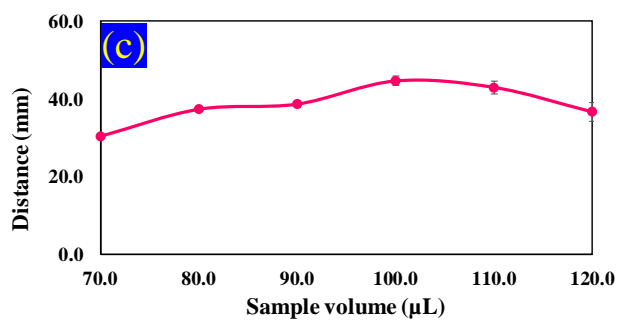
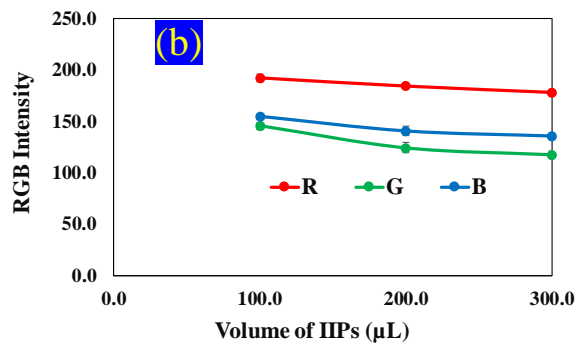
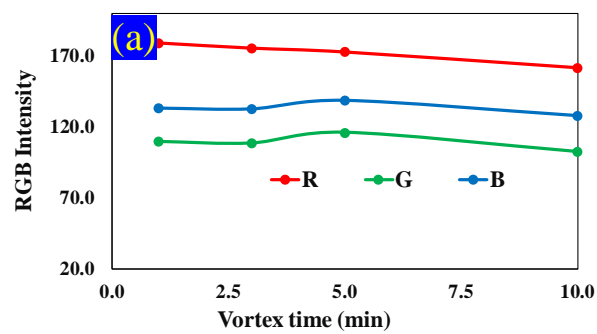


Fig. S8. Graph of optimization studies of (a) vortex time, (b) volume of IIPs, (c) sample volume, and (d) time.



Fig. S9. Image of IIPs-based dTADs sensor for Zn (II) detection at 1.0 mg L⁻¹.